Available online at www.sciencedirect.com
ScienceDirect
Energy Reports 9 (2023) 154–162
www.elsevier.com/locate/egyr

The 7th International Conference on New Energy and Future Energy Systems (NEFES 2022), 7th NEFES, 25-28 October 2022, Nanjing (virtually), China

Design and realization of a 200 A low-cost high-side switch for automotive applications

Annunziata Sanseverino[a,*], Carmine Abbate[b], Lucio Colella[b], Roberto Di Folco[b], Emanuele Martano[a], Francesco Velardi[a]

[a] DIEI, University of Cassino and Southern Lazio, Via Di Biasio 43, 03043 Cassino, Italy
[b] DAC Engineering and Research srl, Via San Giovanni Battista, 2, 03037, Pontecorvo, Italy

Received 20 February 2023; accepted 1 March 2023
Available online xxxx

Abstract

The realization of a high side power switch for driving a motor with a load current of 200 A in a hostile environment is presented. For such high currents currently electromechanical devices are used which have reliability and wear problems when working in environments with high temperature and humidity. The proposed solution was developed by connecting in parallel five commercial switches mounted on an FR4 support. An accurate thermal design, aided by finite element analysis, made it possible to avoid the use of an external heat sink, thus minimizing the weight and cost of the assembled circuit. Experimental tests under actual operating conditions have demonstrated the reliability of the proposed solution.

Peer-review under responsibility of the scientific committee of the 7th International Conference on New Energy and Future Energy Systems, NEFES, 2022.

Keywords: Parallel connection; Finite element analysis; Power static switch

1. Introduction

A power switch is a device used to connect/disconnect a load from the power supply. The load can be positioned below or above the switch, giving rise to the so-called low-side and high-side configurations. The high-side configuration requires the switch to be placed between the power supply and the load and is the preferred switching technique when shorts to ground are more likely to occur, in which case it is safer to disconnect the load from the battery rather than from the ground.

Regardless of the topology, the switch can be electromechanical, relay, or electronic, i.e. based on the switching operation of an active device. Electromechanical relays are very simple devices that use moving contacts, driven by a low-voltage signal that closes the power supply circuit. However, the presence of a moving part limits the life of these devices as it makes them subject to wear, deformation and corrosion, especially when they operate in environments with high temperatures and humidity.

* Corresponding author.
E-mail address: a.sanseverino@unicas.it (A. Sanseverino).

https://doi.org/10.1016/j.egyr.2023.03.005

Peer-review under responsibility of the scientific committee of the 7th International Conference on New Energy and Future Energy Systems, NEFES, 2022.

Solid State Relays (SSRs) are more expensive but, having no moving parts, they guarantee greater reliability and therefore are replacing electromechanical devices in many fields of application. A further advantage of SSRs lies in the fact that it is possible to integrate in the same device, in addition to the switching function, the driving circuits, the circuits for diagnostics [1] and protection [2]. The result is the Smart Low-Side and High-Side Switches available for applications in the industrial and automotive sectors. These are devices suitable for inductive, capacitive and resistive loads with excellent robustness and which integrate protection against overload, overvoltage, short circuits, overtemperature, earth leakage, power loss and electrostatic discharge.

These switches manage loads with nominal currents in the tens of Amperes, as the current capacity increases there are no alternatives to the use of electromechanical devices despite the reliability problems that arise if you work in a hostile environment.

The purpose of this work is to propose a possible implementation of a high-side static switch that manages loads with currents higher than hundreds of Amperes. The proposed device was used to replace the electromechanical actuator of the motor of a forklift truck powered at 12 V with a load current of 200 A which works in an environment where the temperature can reach 80 °C with a high level of humidity.

To most used technique to increase the current capacity of a circuit is to realize a multichannel structure by connecting several devices in parallel. This topology is widely exploited for the construction of monolithic switches and guarantees, in addition to the increase in the current range, greater efficiency in terms of area [3] compared to a multichip solution [4]. However, the integration of the individual devices makes it necessary to redesign the protection and diagnostic circuits. A fastest and cheapest solution could be to connect commercial Smart Hide Side Switches in parallel on a standard FR4 support, in order to take advantage of the features already present in the SSR and integrate a control logic on the chip for the management of the protection and diagnostics signals of the individual stages.

In this paper we have explored this possibility by obtaining a circuit that meets the design requirements. With the help of electrical and thermal simulations it was possible to realize a circuit that does not require an external heat sink and therefore has a cost and a reduced footprint, an important requirement in our application. Experimental tests have confirmed the functioning and reliability of the proposed solution.

2. Circuit implementation

The proposed circuit was made by connecting low-cost commercial switches in parallel. The devices are 5 Infineon Technologies BTS50010-1TAE Smart High-Side Switches [5], which are designed to drive currents up to 40 A in 12 V powered systems. Each device integrates a static power switch in silicon with the relative driver, an active clamp system for the absorption of inductive energy, a circuit for measuring the current with relative protection circuit, a voltage and temperature sensors. The driver contains an outward logic interface section that allows both to apply the galvanically isolated on/off logic signal and to make a voltage proportional to the operating current of the device available externally (IS). In conditions of switch anomaly, overcurrent, overvoltage or overtemperature, the IS signal is fixed at the high value corresponding to the fault of the device.

To acquire the IS signals supplied by the individual devices, a control logic based on a microprocessor (data logger) housed on the PCB has been designed. This circuit permits to evaluate the distribution of currents in the individual branches, which is a crucial problem when connecting multiple devices in parallel and to measure the temperature by acquiring data from a sensor placed near the switches. The data logger, being a programmable circuit, can be configured to signal anomalies to the user and interface with the on-board electronics.

The switches are mounted on the PCB using circular symmetry with an angular spacing of 22.5° and with a distance between the centres of the devices of 13 mm. The spacing angle was determined taking into account the arrangement of the power paths on the left of the PCB which left an angle of 90° free giving rise to 4 interspaces of 22.5 degrees each. The connection tracks of the outputs of the individual devices have been made as short as possible and with the same length. This device, together with the circular symmetry, contributes to a homogeneous distribution of the currents. In series with each switch a 40 A fuse was placed. The fuses intervene in the event of a short circuit in one or more devices allowing the switch to open.

The PCB layout was made using Altium Designer. Fig. 1 shows a view of the board with the vias of the upper face highlighted in red and that of the lower face in blue. It shows the arrangement of the devices with the relative fuses, the area where the data logger is mounted and a section (on the right) dedicated to the positioning of the external connector and further protection circuits.

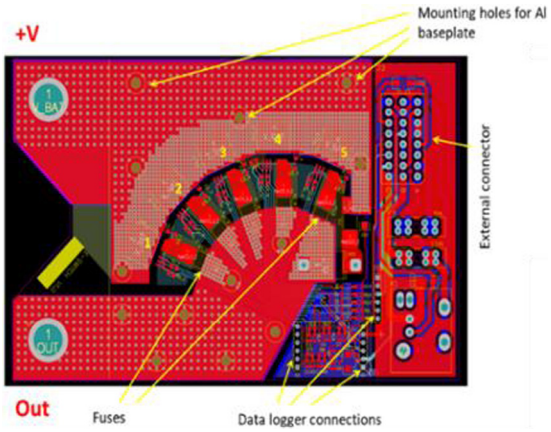

Fig. 1. PCB view. (For interpretation of the references to colour in this figure legend, the reader is referred to the web version of this article.)

The current, starting from V_BAT, flows towards the power switches and the relative fuses, is collected with circular symmetry and conveyed to the power output terminal OUT. On the right we have a standard connector for automotive application that communicates with the data logger and with the vehicle.

In addition to the placement of the devices, the design of the PCB required the definition of the vias and the management of the heat dissipation produced by the switches and fuses. The latter have an internal resistance of 1.3 mΩ which, at the rated current of 40 A, produces a dissipated power for each fuse of 2.1 W at ambient temperature $T_{AMB} = 25$ °C [6]. However, this value is destined to increase as the circuit must work at a higher ambient temperature at which the internal resistance of the fuse increases, leading to an increase in the dissipated power.

For the definition of vias, which represent the path of electrical and thermal energy, numerous articles propose guidelines based on simulations, analytical models and experimental evaluations [5,7–10].

Starting from these general criteria, the determination of the number, size and positioning of the thermal channels has been optimized with the aid of a software capable of performing a thermal analysis of the circuit in the various operating conditions and with different values of the ambient temperature. As can be seen from Fig. 1, the vias thicken in correspondence with the cases of the devices, creating a matrix structure with the distance between the vias of 1.2 mm and the size of the single vias of 0.7 mm. Each vias connects the 4 layers of the support.

The thermal simulations, reported in the following paragraphs, also showed that to keep the system temperature below the maximum operating temperature, during the operation time, it is necessary to use an additional thermal capacity. For this purpose, two 5 mm thick Aluminium plates were mounted on the bottom of the PCB using the fixing holes highlighted in Fig. 1. The shape of these two plates, shown in Fig. 2, exactly overlaps the path of electrical conduction.

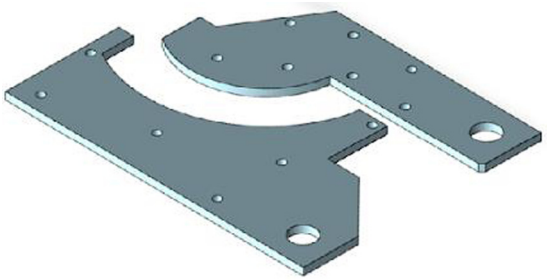

Fig. 2. 3D view of the Al plates mounted on the PCB bottom.

3. Electrical and thermal simulations

Before carrying out a thermal analysis of the circuit, electrical simulations were performed using a software distributed by Infineon which allows to estimate the junction temperature and the power dissipated by the single device in different operating conditions. The software allows to simulate the behaviour of the device mounted on a PCB taking into account the parameters of the support, the load and connections providing several outputs: the voltage proportional to the output current (IS), the output current (Iout), the junction temperature (TJ), the output voltage (VS) and the power supply (VOUT). The parameters used in the simulations, which reproduce the characteristics of the PCB and the operating conditions of the switch, are collected in Table 1.

Table 1. Electrical and technological parameters used in simulation in nominal conditions.

PCB	
Dielectric	FR4
No of layer	4
Total thickness	0.8 mm
External copper thickness	105 μm
Internal copper thickness	35 μm
External FR4 thickness	0.13 μm
Internal FR4 thickness	0.5 μm
Connection cables	
Resistance	2 mΩ
Inductance	18 μH
Load	
Resistance	20 mΩ
Inductance	95 μH

The first test reproduced the operating conditions: $T_{AMB,MAX} = 80$ °C, $I_{NOM} = 40$ A, switch-on time $t_{ON} = 20$ s. The results, reported in Fig. 3, show that the maximum junction temperature reaches 100 °C in correspondence of $t = 20$ s. The total power dissipated under nominal conditions has been estimated about 3 W.

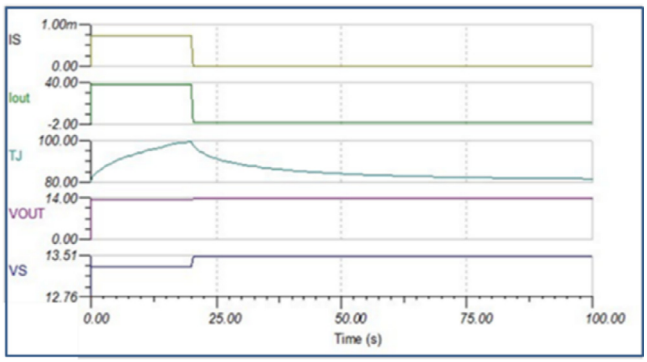

Fig. 3. Simulated electrical parameters for a single device @ $I_{NOM} = 40$ A, $T_{AMB,MAX} = 80$ °C, $t_{ON} = 20$ s.

Subsequently the value of the load resistance was modified to analyse the behaviour of the device under overload conditions. For currents $I = 50$ and 60 A, the junction temperature TJ reaches 115 and 133 °C respectively.

The thermal simulations were carried out in a COMSOL Multiphysics environment [11] and involved the entire circuit. The first step was the creation of a solid model of the PCB using the parameters of Table 1 and inserting the electronic components as planned. The PCB was placed inside a ULTRAMID A3K plastic case. The simulation mesh was obtained by dividing the entire geometry into infinitesimal elements, each with its own chemical–physical characteristics.

Ten thermal sources were considered on the PCB: 5 active devices and 5 fuses. The ambient temperature was set at 80 °C and an emission of thermal energy by the heat sources was assumed for a duration of 20 s. The thermal energy was fixed based on the electrical simulations assuming a current of 40 A in each device and knowing the dissipation parameters of the fuses. Subsequently the heat source was turned off and the conductive and convective heat flux that occurs inside the circuit was analysed.

Fig. 4 shows the simulated PCB and the external case, the black circles represent the points where the temperature was monitored. The red circles, labelled with alphabetic letters, highlight the most significant points that correspond to the heat sources (C and D), the board (E) and the case (A, B).

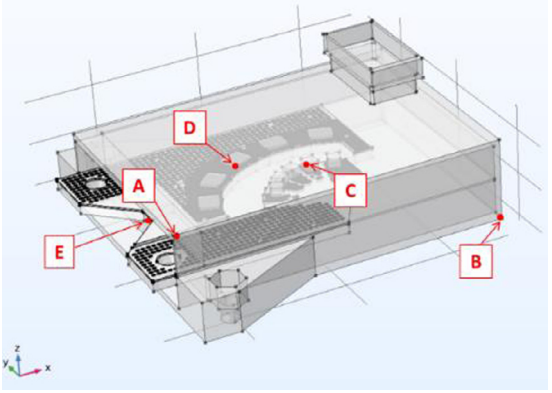

Fig. 4. Simulated structure. The grey and red dots indicate the position of the temperature probes. (For interpretation of the references to colour in this figure legend, the reader is referred to the web version of this article.)

Several simulations were carried out to test the effectiveness of the aluminium plates and the possible filling of the cavity with epoxy resin to favour heat dissipation. The test conditions are summarized in Table 2.

Table 2. Test conditions for COMSOL simulations.

Case study	Al baseplate	Epoxy resin X238	Air
I	×	×	
II	×		×
III			×
IV		×	

For each test condition, thermographic images at different times were obtained. Fig. 5 shows an example of a thermographic image of the PCB obtained for case II, Al baseplate and the cavity in air, at $t = 20$ s. The maximum temperature detected on the PCB was 86.5 °C reached in correspondence of the fuses.

Table 3 report the maximum temperature detected for all test conditions. The presence of the baseplate (case I and II) favours the dissipation of heat but as shown below, other things being equal, the use of the epoxy resin (case I) makes the cooling faster.

Fig. 6 shows the temperature as a function of time evaluated in correspondence of the red dots of Fig. 5 for the case I. As expected, the temperature reaches its maximum value after 20 s at the fuse (C), the devices and vias (D and E) are at a few degrees lower while the case remains at ambient temperature.

The curve relating to point C is compared in Fig. 7 with the corresponding one obtained for the case II. The peak value is very similar in the two cases but the epoxy resin favours heat dissipation: in case I the structure reaches 81.5 °C after about 100 s, in case II after 500 s.

The results of the thermal simulations guided the realization of the prototype presented in the following paragraph.

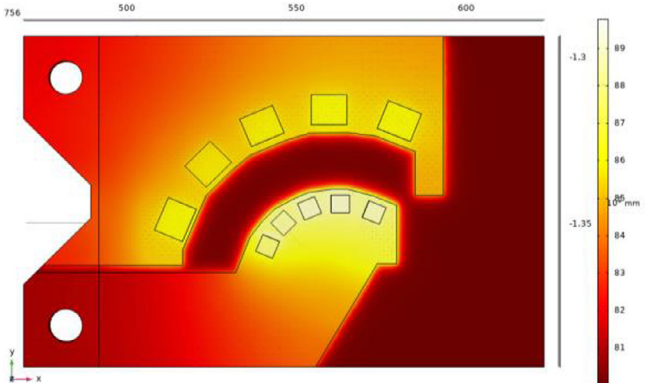

Fig. 5. Simulated temperature distribution for case II @ $T_{AMB,MAX} = 80$ °C, $t = 20$ s. (For interpretation of the references to colour in this figure legend, the reader is referred to the web version of this article.)

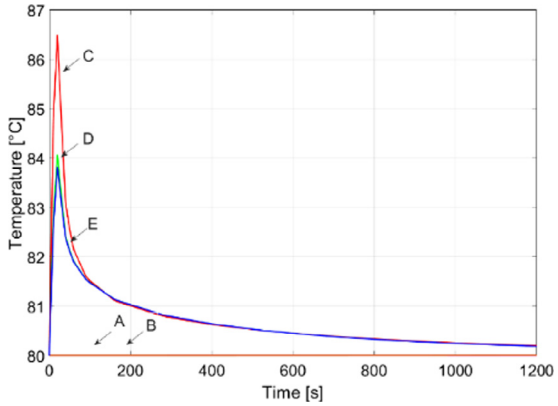

Fig. 6. Simulated temperature versus time for case study I (dots A to E of Fig. 5).

Table 3. Simulated maximum temperature for the different test conditions.

Case study	T_{MAX} [°C]
I	86.5
II	86.3
III	112
IV	101

4. Experimental results

Fig. 8 shows the detail of the realized PCB. The top view (Fig. 8a) points out the devices arranged in a radial pattern with the relative fuses in series, the data logger card, the external interface connector, an auxiliary relay with the relative protection fuses. We also find the power contacts and the screws for anchoring the Al baseplate which is clearly visible from the bottom view of Fig. 8b.

The tests on the proposed device were performed using circuit diagram shown in Fig. 9. In addition to the power section, the circuit includes an enabling circuit for the individual switches (Driver), the V_{CC} power supply and the load. The first tests were carried out using as load an RL network, that simulates the DC motor. The inductance was set at L = 75 μH while the resistance was modified to study the behaviour of the circuit for different values of the output current. The prototype was connected to a laptop to interface the data logger and display the monitored parameters on the screen.

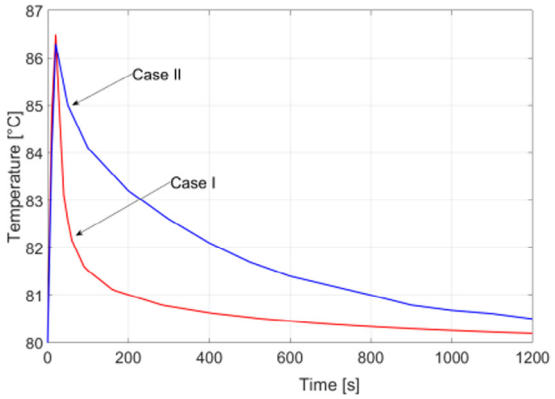

Fig. 7. Fuse temperature versus time for test conditions I and II.

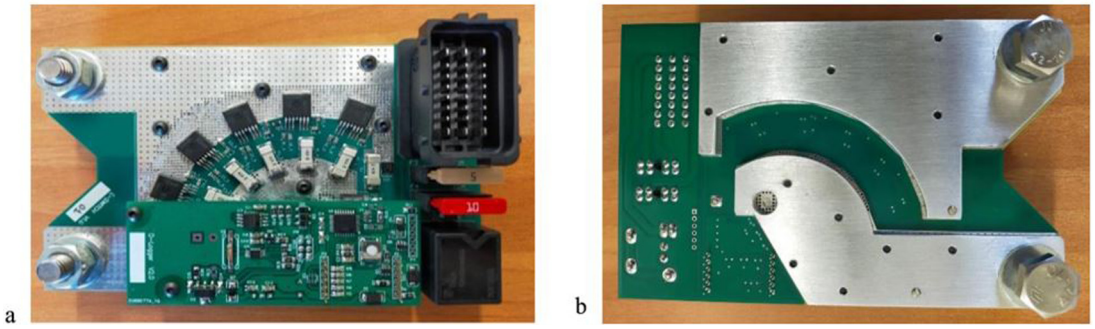

Fig. 8. (a) Top and (b) bottom view of the realized PCB.

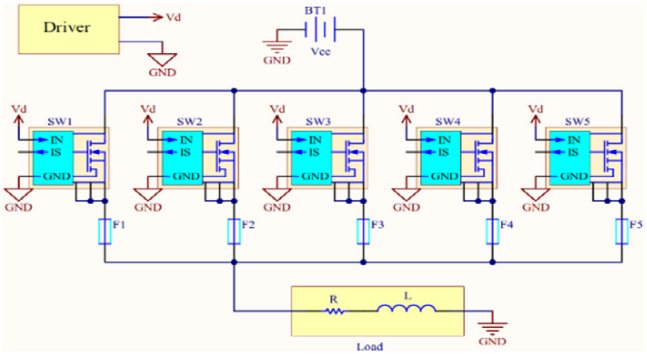

Fig. 9. Schematic of the experimental set-up.

The first step was to monitor the current distribution and temperature on the PCB using a FLIR thermal imaging camera. The tests were performed at $T_{AMB} = 12$ °C due to the difficulty of positioning the camera in a controlled temperature environment.

The device, powered with Vcc = 13.8 V, was turned on for 20 s and thermal images were acquired. During these tests R_{LOAD} was varied until reaching the overload current of 285 A. Table 4 summarizes the test conditions, the value of the output current and the maximum temperature detected in each condition.

Fig. 10 shows the thermographic images at $t = 20$ s in the case of rated current $I = 200$ A (Fig. 10a) and in the case of overload with a current increase of about 40% (Fig. 10b).

Table 4. Measured output current and maximum temperature on PCB for different test conditions.

Test	R_{LOAD} [mΩ]	I [A]	T_{MAX} [°C]
1	250	51	17.8
2	125	100	21.2
3	90	141	28.4
4	60	200	40.8
5	50	235	60.7
6	40	285	139.0

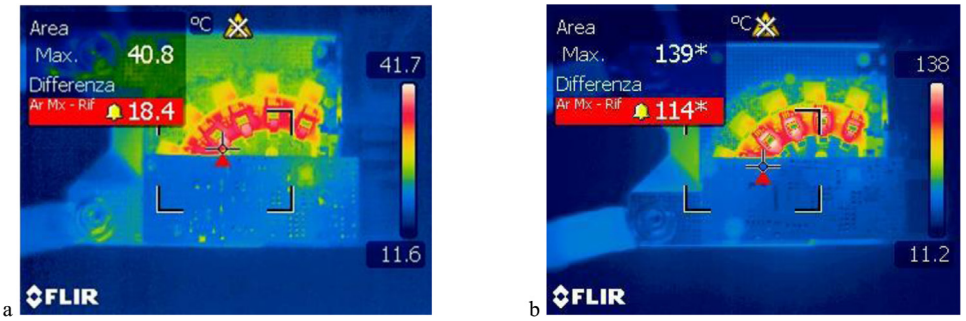

Fig. 10. Temperature distribution @ $t = 20$ s for (a) test # 4 and (b) test # 6.

The results show, for both cases, a homogeneous distribution of the current which is confirmed by the measurements acquired with the data logger which report a maximum dispersion of 5% between the single devices. The temperature increases with the current with quadratic law up to $I = 235$ A reaching in nominal conditions $T_{MAX} = 40.8$ °C in correspondence with the fuse, subsequently a much more pronounced increase is observed.

The drastic increase in temperature is attributable to the fuse for which the increase in current beyond its nominal value produces an increase in temperature with a consequent increase in its internal resistance. An unstable phenomenon is established which, if it persists, leads to the fuse opening.

The prototype was subsequently tested in real operating conditions. The RL network has been replaced by the forklift motor and the circuit was inserted inside a climatic chamber at a temperature of 80 °C and with a humidity of 30%. Switching took place under the maximum load conditions specified by the user.

Fig. 11a shows the detail of the turn on in which there is an inrush overcurrent that reaches 353 A stabilizing at 273 A. The turn off is shown in Fig. 11b. In this case there is an overvoltage due to the stray inductance of the motor. The maximum overvoltage measured was 33 V which corresponds to the clamp voltage of the transient voltage suppressor diode 15KPA18A inserted as the protection circuit.

The last test carried out had the purpose of verifying the reliability of the system, the switchings in the climatic chamber were repeated with on and off cycles ton = 20 s and toff = 20 min, as per specification, for a total duration of 720 h without the data logger has shown malfunctions.

5. Conclusion

The feasibility of a high-side power switch for loads working with high currents has been accessed. The switch was realized by connecting low-current commercial smart devices in parallel in order to take advantage of the features present in the individual devices. This made it possible to simplify the design of the switch which focused on the arrangement of the devices on the printed circuit and on the analysis of the thermal performance, obtaining a circuit that does not require the use of external heat sinks with consequent low cost and reduced size.

Preliminary tests conducted on real load show that the system is well within the design specifications and that it can switch currents up to 300 A if the current capacity of the fuses is increased.

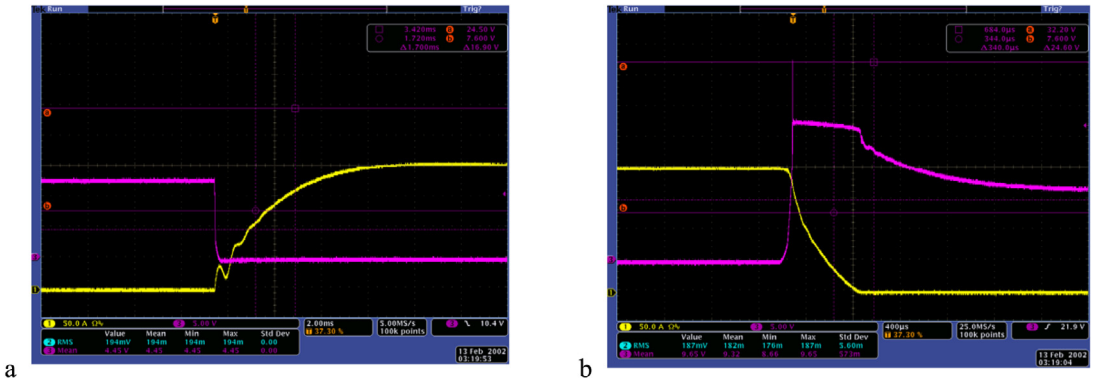

Fig. 11. Measured waveforms at (a) turn-on and (b) turn-off under operating condition. The yellow curves represent the output current, in purple the voltage across the power contacts. $T_{AMB} = 80$ °C, humidity 30%. (For interpretation of the references to colour in this figure legend, the reader is referred to the web version of this article.)

Declaration of competing interest

The authors declare that they have no known competing financial interests or personal relationships that could have appeared to influence the work reported in this paper.

Data availability

No data was used for the research described in the article.

References

[1] Davis B, Wellnitz K. Intelligent diagnostic features available for high side power switching. In: Proceedings of 1994 IEEE workshop on power electronics in transportation. 1994, p. 23–31.
[2] Terçariol WL, Saez RLT, Nascimento ICR. High and low side high voltage switch with over voltage and over current protection. In: 2013 IEEE computer society annual symposium on VLSI. ISVLSI, 2013, p. 177–81.
[3] Harmouch M. High-Side switches paralling channels. Texas Instruments Application Report SLVA949-2018.
[4] Danchiv A, Hulub M, Manta D. An area efficient multi-channel high side switch implementation. In: 2011 Proceedings of the ESSCIRC. ESSCIRC, 2011, p. 327–30.
[5] https://www.infineon.com/cms/en/product/power/smart-low-side-high-side-switches/high-side-switches/power-profet-automotive-smart-high-side-switch/bts50010-1tae/.
[6] https://www.littelfuse.com/products/fuses/surface-mount-fuses/nano-2-fuses/456sd.aspx.
[7] Shen Y, Wang H, Blaabjerg F, Zhao H, Long T. Thermal modeling and design optimization of PCB vias and pads. IEEE Trans Power Electron 2020;35(1):882–900.
[8] Catalano AP, Trani R, Scognamillo C, d'Alessandro V, Castellazzi A. Optimization of thermal vias design in PCB-based power circuits. In: 2020 21st International conference on thermal, mechanical and multi-physics simulation and experiments in microelectronics and microsystems (EuroSimE). 2020, p. 1–5.
[9] Anand V, Singh V, Ladwal VK. Study on PCB designing problems and their solutions. In: 2019 International conference on power electronics, control and automation. ICPECA, 2019, p. 1–5.
[10] Asghari T. PCB thermal via optimization using design of experiments. In: Thermal and thermomechanical proceedings 10th intersociety conference on phenomena in electronics systems, (2006). ITHERM 2006. 2006, p. 224–8.
[11] COMSOL Multiphysics® V. 6.0. www.Comsol.Com.. Stockholm, Sweden: COMSOL AB.